Alternative designs and tropical tree seedling growth performance landscapes

Samantha J. Worthy [iD],[1,6] Daniel C. Laughlin,[2] Jenny Zambrano [iD],[3] María N. Umaña [iD],[4] Caicai Zhang,[5] Luxiang Lin,[5] Min Cao,[5] and Nathan G. Swenson[1]

[1]*Department of Biology, University of Maryland, 1210 Biology Psychology Building, 4094 Campus Drive, College Park, Maryland 20742 USA*
[2]*Department of Botany, University of Wyoming, Laramie, Wyoming 82071 USA*
[3]*The School of Biological Sciences, Washington State University, Pullman, Washington 99164 USA*
[4]*Department of Ecology and Evolutionary Biology, University of Michigan, Ann Arbor, Michigan 48109 USA*
[5]*CAS Key Laboratory of Tropical Forest Ecology, Xishuangbanna Tropical Botanical Garden, Chinese Academy of Sciences, Kunming, Yunnan 650201 China*

Abstract. The functional trait values that constitute a whole-plant phenotype interact with the environment to determine demographic rates. Current approaches often fail to explicitly consider trait × trait and trait × environment interactions, which may lead to missed information that is valuable for understanding and predicting the drivers of demographic rates and functional diversity. Here, we consider these interactions by modeling growth performance landscapes that span multidimensional trait spaces along environmental gradients. We utilize individual-level leaf, stem, and root trait data combined with growth data from tree seedlings along soil nutrient and light gradients in a hyper-diverse tropical rainforest. We find that multiple trait combinations in phenotypic space (i.e., alternative designs) lead to multiple growth performance peaks that shift along light and soil axes such that no single or set of interacting traits consistently results in peak growth performance. Evidence from these growth performance peaks also generally indicates frequent independence of above- and belowground resource acquisition strategies. These results help explain how functional diversity is maintained in ecological communities and question the practice of utilizing a single trait or environmental variable, in isolation, to predict the growth performance of individual trees.

Key words: demographic rate; forest ecology; functional traits; growth; seedlings; tropical forest.

Introduction

The diversity and dynamics of communities are driven by differential demographic rates that largely arise from how phenotypes interact with the environment (Fonseca et al. 2000, Ackerly 2003, Cavender-Bares et al. 2004, HilleRisLambers et al. 2012, Anderson 2016). The links between functional traits, demographic rates, and population and community structure form the basis of trait-based community ecology (McGill et al. 2006). In this regard, two analytical approaches are common: quantifying the relationships between single traits and demographic rates, and quantifying the relationships between traits and environmental gradients (Wright and Westoby 1999, Poorter et al. 2008, Enquist et al. 2015, Jager et al. 2015, Costa et al. 2017). The first approach generally operates under the implicit assumption that trait–demographic-rate relationships are consistent across

environments (Wright et al. 2004, Poorter et al. 2008, Kraft et al. 2010, Adler et al. 2014). For example, a low wood density confers fast growth (e.g., Chave et al. 2009, Kraft et al. 2010). The second approach implicitly assumes the optimal value for a given trait changes across an environmental gradient. Thus, the two approaches appear to be inconsistent, with the first searching for a single global optimum and the second searching for a shifting optimum across an environmental gradient (Laughlin et al. 2018).

The functional diversity in ecological communities can potentially be explained by the existence of alternative designs, i.e., different phenotypic trait combinations that lead to similar demographic performance in a given environment (Marks and Lechowicz 2006). Alternative designs arise when the relationship between a trait and performance is dependent upon an interaction with another trait. These trait × trait interactions can be demonstrated using performance landscapes where one can visualize expected performance along two trait axes (Fig. 1). While performance landscapes are rarely utilized in functional trait-based ecology, evolutionary

a) Low end of environmental gradient　　b) High end of environmental gradient
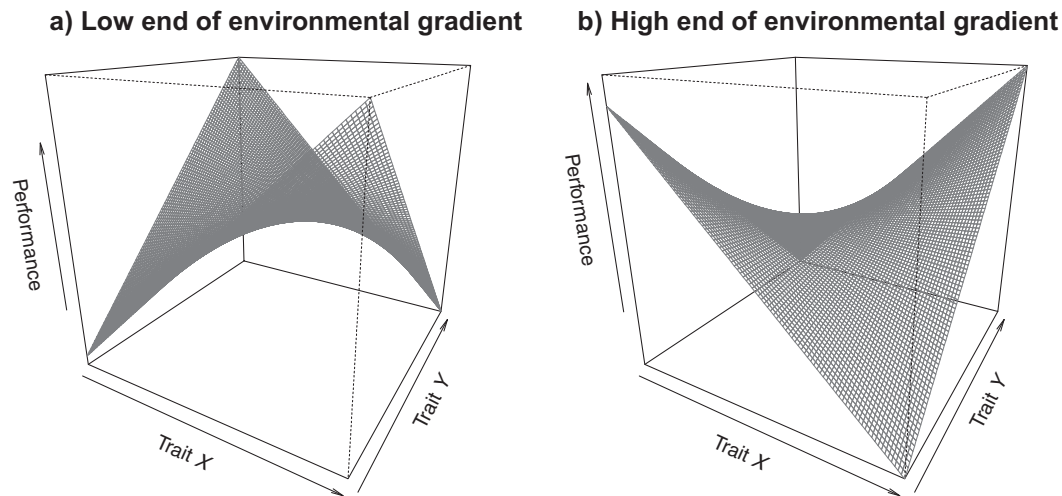

Fig. 1. Conceptual model of a theoretical performance landscape of an individual along two trait axes at (a) the low end of an environmental gradient and (b) at the high end of an environmental gradient. Note the multiple performance peaks within an environment and the shift in location of these performance peaks across the environmental gradient.

biologists have long utilized these landscapes beginning with Wright's adaptive landscape of gene frequencies (Wright 1931, 1932, 1945), progressing from Simpson's phenotypic landscape (Simpson 1944) to adaptive landscapes (Arnold et al. 2001). Despite this existing literature and the recognition for decades that plant-functional-trait-based ecology should focus more intently on trait × trait interactions (Ackerly et al. 2000, Marks and Lechowicz 2006, Dwyer and Laughlin 2017a, D'Andrea et al. 2018), performance landscapes have been largely ignored (but see Laughlin and Messier 2015, Dwyer and Laughlin 2017b) as has a focus on individual-level positions on these landscapes over that of species means.

Functional diversity within a community can be further promoted if the shape of performance landscapes shifts along local-scale environmental gradients. In other words, the alternative phenotypic designs that perform best on one end of a local-scale environmental gradient will not necessarily be those expected to perform best on the other end thereby increasing the diversity of traits and trait combinations performing well within a community (Fig. 1). Thus, not only do trait × trait interactions need to be considered when modeling individual performance, but a simultaneous investigation of the interactions among multiple traits and environmental gradients may be necessary to understand how traits drive performance and plant community diversity.

Theory indicates that trait × trait and trait × environment interactions are essential for understanding how traits relate to whole-plant performance, influence population level parameters, and drive community structure and dynamics (Marks and Lechowicz 2006, Enquist et al. 2015). However, we currently lack clear empirical evidence that multiple phenotypic optima exist in a given environment and that these optima change across an environmental gradient. Ideally, such evidence would be gathered using individual-level trait, demographic, and environmental information to account for the importance of intraspecific trait variation (Yang et al. 2018, Swenson et al. 2020). Here, we determined whether interactions between multiple functional traits and environmental gradients impacted tropical tree seedling growth rates. Specifically, we modeled the growth of 1,559 individual tree seedlings from 122 species in a Chinese tropical rainforest using an unprecedented data set of individual-level leaf, root, and stem trait data and detailed light and soil nutrient data. We asked two main questions: (1) Do alternative phenotypic designs have similar demographic outcomes within an environment? And (2) how do the peaks and ridges of growth performance landscapes change across environmental gradients? We focus on seedlings because differential demographic rates at the seedling stage have large and lasting impacts on tropical forest structure and dynamics (Metz et al. 2010, Paine et al. 2012, Green et al. 2014, Umaña et al. 2016).

METHODS

Study site

This study was conducted in a tropical rainforest in Xishuangbanna, which is in the Chinese province of Yunnan (101°34′ E, 21°36′ N). The climate for this region is monsoonal with a mean annual temperature of 21.8°C, mean annual precipitation of 1,493 mm, and soil pH between 4.5 and 5.7 (Cao et al. 2008). There are two seasons in this forest, differentiated by precipitation patterns, where the dry season starts in November and ends in April and 85% of the precipitation occurs between May and October (Cao et al. 2008).

Seedling plot establishment and monitoring

Across 2-ha of forest, 215 1 × 1 m² seedling plots were installed in a regular grid. All seedlings from germination to 50 cm in height were tagged, identified, and monitored for 1 yr from 2013 to 2014. Seedlings were monitored for survival monthly, but height was measured twice, once at the beginning and once at the end of the census period. During our study, the average temperature was 22.4°C and the total rainfall was 1,590 mm. At the end of the year-long monitoring, all surviving seedlings were harvested for functional trait measurement. In total, there were 1,559 seedlings of 122 species distributed across the 215 plots. The number of seedlings varied from 1 to 33 across the plots with a mean number of 7.25 individuals and 1.76 species per plot.

Functional traits

Seven functional trait measurements were taken on each individual seedling in the study (Appendix S1: Table S1). The organ-level traits measured were leaf mass per unit area (LMA) and mean leaf thickness, which were measured on one to three leaves for each individual. The biomass allocation traits measured in this study were leaf area ratio (LAR; total plant leaf area divided by whole-plant dry mass), leaf mass fraction (LMF; total leaf dry mass divided by whole-plant dry mass), root mass fraction (RMF; total root mass divided by whole-plant mass), stem mass fraction (SMF; total stem dry mass divided by whole-plant dry mass), and stem specific length (SSL; stem length divided by dry stem mass), all according to (Poorter et al. 2012) and previously reported in (Umaña et al. 2015). Leaves, roots, and stems were manually separated in the lab using hand pruners and dried in the oven for 72 h at 70°C. These traits were chosen for measurement because they represent major allocation trade-offs at the organ and whole-plant levels that should impact growth performance. Specifically, LMA represents the leaf economics spectrum (Reich et al. 1997, Wright et al. 2004) where species with high LMA have a conservative strategy with long leaf lifespans, but lower mass-based photosynthetic rates and species with low LMA values have a more acquisitive strategy with short leaf life spans and higher mass-based photosynthetic rates. Leaf thickness is measured to indicate leaf mechanical resistance to damage (Onoda et al. 2011). LAR and LMF reflect relative allocation to leaf tissue and combined with LMA are often used in models of plant growth in functional ecology (Garnier 1991, Enquist et al. 2007, Poorter et al. 2012). RMF, SMF, and SSL are indicative of allocation to non-photosynthetic tissue. RMF and LMA were of particular interest to us as previous work has indicated that they both are highly responsive to soil nutrient and light gradients (Freschet et al. 2015). Higher RMF and higher LMA values indicate an allocation pattern that maximizes soil resource gain relative to light resource gain.

Thus, we might expect high RMF and LMA values for individuals in poor soils and/or in shade tolerant individuals and the opposite pattern in nutrient rich soils and/or in high light environments.

Environmental variables

Local environmental conditions were characterized by measuring soil nutrients and light availability for each plot. Prior research has shown that these environmental variables vary significantly, even at local scales (Hubbell et al. 1999, Baldeck et al. 2013, Umaña et al. 2018). Percent canopy openness, measured using hemispherical photographs taken systemically with a Nikon FC-E8 lens and a Nikon Coolpix 4500 camera (Tokyo, Japan), was used to determine light availability. We do note that these measurements only capture canopy openness and, therefore, do not capture individual plant light environments or changes in light environments through time, but they do offer a quick and pragmatic approach for estimating the average light environment in a sample plot. Photographs were taken with the camera 1 m above the ground before sunrise with cloudy conditions between March and April 2014 for each seedling plot. The images were analyzed using Gap Light Analyser software (Appendix S1: Table S2; software *available online*).[7]

We also measured soil nutrients for each of the plots due to prior research showing relationships between soil nutrients, habitat associations and demography (Itoh et al. 2003, Palmiotto et al. 2004, Russo et al. 2005, 2008, John et al. 2007). To analyze soil nutrients, 50 g of topsoil (0–10 cm in depth) was collected from each of the corners of the plot. After being air dried and sifted, the cation availability was determined using the Mehlich III extraction method and atomic emission inductively coupled plasma spectrometry (AE-ICP). Total nitrogen (N) and carbon (C) content were determined by total combustion using auto-analyzer and pH measured with a pH meter. All soil analyses were conducted at the Biogeochemical Laboratory at Xishuangbanna Tropical Botanical Garden (Appendix S1: Table S2).

All functional trait and environmental variables were natural log-transformed and scaled to a mean of 0. The dimensionality of the soil data was reduced using a principal component analysis (PCA) (Appendix S1: Fig. S1). The first three orthogonal axes, explaining 78% of the total soil variation, were used for further analyses (Appendix S1: Table S3). PC1 scores were negatively associated with K, Mg, and Zn, which are known to play major roles in photosynthesis, growth, as well as seed and stem maturation (Terry and Ulrich 1974, Broadley et al. 2007, Holste et al. 2011). PC2 scores were negatively associated with Ca and P. Soil phosphorous is the major limitation of these two elements as phosphorous

---

[7] http://www.caryinstitute.org/science-program/our-scientists/dr-charles-d-canham/gap-light-analyzer-gla

deficiency is known to have negative impacts on plant growth (Wissuwa 2003, Wright et al. 2004). PC3 scores were negatively associated with C and N. Soil N is of particular interest as N is a key component of RuBisCO and, therefore, a resource that can limit photosynthesis (Evans and Clarke 2019).

Quantifying growth rates

To determine the relative growth rate (RGR) of each seedling, the change in log-transformed height was calculated for each individual as

$$\mathrm{RGR} = (\log(M_{t+\Delta t}) - \log(M_t))/\Delta t.$$

The variable M is the height at successive time steps t (Hoffmann and Poorter 2002). A value of 1 was added to all observed RGR values and then the data were ln-transformed and scaled to a mean of 0 to approximate normality (Appendix S1: Table S1).

Linear mixed-effects model description

We built linear mixed-effects models of growth using a Bayesian approach ranging in complexity from a single term to having a three-way interaction with a focus on addressing the biological question of whether trait × trait, trait × environment, or trait × trait × environment interactions, which are frequently not considered, influence growth rates. Models were run for all pairwise combinations of the seven functional traits and environmental variables for a total of 84 models. In all models, RGR followed a lognormal distribution:

$$\log \mathrm{RGR}_i \sim N(z_i, \sigma_z),$$

where z_i was the relative growth rate of each individual, σ_z was the variance, and i was each individual. First, individual linear models were fit where RGR was a function of a single trait and initial seedling size, where z_i was the relative growth rate of each individual, α was the model intercept, $\beta1_p$ and $\beta2_j$ were the plot and species random effects, respectively, $\beta3$ was the effect of a trait, and $\beta4$ was the effect of initial size

$$z_i = \alpha + \beta1_p + \beta2_j + \beta3 \times \mathrm{trait} + \beta4 \times \mathrm{initial\ size}. \quad (1)$$

These simple linear models highlight a common method used to link functional traits, demographic rates, and population and community structure in the functional trait literature. In rare instances, a functional trait and the environment have been combined in models to include their interactive effect as both impact plant performance (Laughlin and Messier 2015, Dwyer and Laughlin 2017b, Blonder et al. 2018). To mimic these models, we modeled the linear predictor, RGR, using mixed-effects models including a two-way interaction between a functional trait and an environmental variable. Models were of the general form

$$\begin{aligned} z_i =\ & \alpha + \beta1_p + \beta2_j + \beta3 \times \mathrm{trait} + \beta4 \times \mathrm{environment} \\ & + \beta5 \times \mathrm{initial\ size} + \beta6 \times \mathrm{trait} \times \mathrm{environment}, \end{aligned}$$

$$(2)$$

where z_i was the relative growth rate of each individual, α was the model intercept, $\beta1_p$ and $\beta2_j$ were the plot and species random effects, respectively, $\beta3$ was the effect of a trait, $\beta4$ was the effect of the environmental variable, $\beta5$ was the effect of initial seedling size, and $\beta6$ was the effect of the interaction between the trait and the environmental variable on RGR.

Last, we modeled RGR using a linear mixed-effects model including a three-way interaction between two functional traits and an environmental variable. The three-way interaction term in these models is included to represent a relationship between a functional trait and growth performance dependent upon another functional trait and the environment. In this model, RGR of each individual was modeled using the general form

$$\begin{aligned} z_i =\ & \alpha + \beta1_p + \beta2_j + \beta3 \times \mathrm{trait}_1 + \beta4 \times \mathrm{trait}_2 \\ & + \beta5 \times \mathrm{environment} + \beta6 \times \mathrm{trait}_1 \times \mathrm{trait}_2 \\ & + \beta7 \times \mathrm{trait}_1 \times \mathrm{environment} + \beta8 \times \mathrm{trait}_2 \\ & \times \mathrm{environment} + \beta9 \times \mathrm{trait}_1 \times \mathrm{trait}_2 \\ & \times \mathrm{environment} + \beta10 \times \mathrm{initial\ size}, \end{aligned} \quad (3)$$

where z_i was the relative growth rate of each individual, α was the model intercept, $\beta1_p$ and $\beta2_j$ were the plot and species random effects, respectively, $\beta3$ was the effect of trait_1, $\beta4$ was the effect of trait_2, $\beta5$ was the effect of the environmental variable, $\beta6$ was the effect of the interaction between trait_1 and trait_2, $\beta7$ was the effect of the interaction between trait_1 and the environment, $\beta8$ was the effect of the interaction between trait_2 and the environment, $\beta9$ was the effect of the three-way interaction between trait_1, trait_2, and the environment, and $\beta10$ was the effect of the initial seedling size on RGR.

In all models, plot ($\beta1_p$) and species ($\beta2_j$) were modeled as normally distributed random intercepts to account for species-level differences in RGR that were unrelated to spatial autocorrelation and the traits, respectively. For the hyperparameters of the random effects, we specified diffuse normal priors: $N(\mathrm{mean} = 0, \mathrm{precision} = 0.01)$. The variance hyperparameters were given diffuse gamma priors: $\mathrm{Gamma}(\mathrm{shape} = 0.1, \mathrm{rate} = 0.1)$. We performed variable selection by comparing "full" models, Eq. 3, with models of all other iterations of variables using deviance information criterion (DIC) to determine the most parsimonious model (Spiegelhalter et al. 2002). Typically, it is thought that DIC is a Bayesian analogue of AIC (Kéry 2010). They have a similar justification, but DIC has wider applicability (Spiegelhalter et al. 2002). The two main differences between AIC and DIC calculations are that the maximum likelihood estimate is replaced with the

posterior mean and the number of parameters is replaced with a data-based bias correction (Gelman et al. 2013). Any model with a DIC value within 5 (ΔDIC < 5) of the lowest value for all models was given consideration (Spiegelhalter et al. 2002, Lesaffre and Lawson 2012). Along with evaluating models with DIC, we assessed the fit of the models by checking the posterior predictive distribution of the fit of the actual data with the fit of an "ideal" data set and computed the Bayesian P value (Gelman et al. 1996). As the Bayesian P value approaches 0.5, simulated data generated from the posteriors should look similar to the observed data indicating a good fit model (Gelman et al. 2013). Evaluating models using DIC and Bayesian P values allowed us to compare less complex, commonly used models, Eq. 1 for one, to our high-dimensional models (Eqs. 2 and 3) to test for overall model fit (Bayesian P value ~ 0.5) and discover instances where more complex models, those containing a three-way interaction, are more parsimonious (ΔDIC < 5) than more simple models lacking a three-way interaction between two traits and the environment. Pearson's product-moment correlation coefficients showed that some traits were weakly correlated (Appendix S1: Table S4). We checked for multicollinearity between traits using variance inflation factor (VIF) analysis to verify that all trait combinations had a VIF < 10 thereby indicating that we can include them together in our models (Ohlemüller et al. 2006, Hair et al. 2014, Enquist et al. 2015; Appendix S1: Table S4).

All models were fit using Markov Chain Monte Carlo (MCMC) sampling techniques in JAGS 4.3.0 (Plummer 2003) interfaced with R v3.3.1 programming language using the rjags (Plummer 2016) and runjags (Denwood 2016) packages (Data S1). We ran six parallel chains with random initial values for 50,000 iterations with a burn-in period of 10,000 iterations. Parameter estimates and 95% credible intervals were obtained from the quantiles of the posterior distribution. Parameters were statistically supported when their credible interval did not overlap zero. Convergence of the MCMC chains was assessed visually in traceplots and using the Gelman-Rubin convergence diagnostic to ensure values were less than 1.1 (Gelman and Rubin 1992).

Assessing growth performance peaks

Two criteria had to be met in order to declare the presence of alternative designs in a growth performance landscape. First, the two-way (trait × trait, trait × environment) or three-way interaction (trait × trait × environment) term in the model had to be statistically supported with 95% credible intervals around the parameter estimate not overlapping zero. Second, the slope of the relationship between the traits and RGR, computed as the first partial derivative of the fitted model, had to switch signs across the range of the environmental variable (Laughlin 2018, Laughlin et al. 2018). A switch in sign indicates that the partial

derivative passed through zero at some point along the environmental gradient. This would be evidence that a "saddle" exists at the intermediate environmental condition, due to the probability surface being pulled downward (Laughlin et al. 2018). To verify that the slope was significantly different from zero, we randomly sampled parameter estimates, with replacement, from the posterior distribution 1,000 times and calculated the slope for each sample to determine 95% confidence intervals (Appendix S1: Table S5).

To understand how the effect of two functional traits on RGR changes across the environmental gradients, simple slopes and intercepts were calculated to visualize partial effects and peaks in growth performance. The minimum and maximum observed values were used as constants for the second trait and environmental variable during the calculation of the simple slopes and intercepts. We also statistically tested for the presence of multiple growth performance peaks at each end of the environmental gradients. We randomly sampled, with replacement, from the posterior distribution 1,000 times from each model. We then calculated each of the simple slopes for each of the 1,000 samples. We then determined the number of times the slopes were different in sign for the two growth performance peaks at the same end of the environmental gradient. An exact binomial test with a probability of success equal to 0.50 was used to test for significant differences. In all cases, a P value of <0.05 indicated the presence of two simple slopes, meaning traits were combining in different ways at the same end of the environmental gradient to achieve higher RGR (Appendix S1: Table S6). If the signs of the mean values of the simple slopes were in the same direction for both growth performance peaks in an environment, we were unable to show a statistical presence of one vs. two peaks. All analyses were performed in R statistical software version 3.3.1 (R Development Core Team 2016).

RESULTS

The models in this study were designed based on biological interactions of functional traits and the environment that are known or predicted in the literature (Wright et al. 2004, Baraloto et al. 2010, Fortunel et al. 2012, Adler et al. 2014, Reich 2014, Freschet et al. 2015, Liu et al. 2016). Eight models, out of 84 total, had evidence of multiple growth performance peaks indicated by a significant three-way interaction in the model and a slope that changed sign along the environmental gradient (Appendix S2). Five models, each with a different three-way interaction term, were the most parsimonious or equally parsimonious based on comparison of DIC values between each "full" model (Eq. 3) and simpler versions of each model (Appendix S2: Tables S1–S5). For the remaining three models, the "full" model was not the most parsimonious overall after variable selection, based on DIC, but was more parsimonious than commonly used models, trait × growth rate and

trait × environment × growth rate (Appendix S2: Tables S6–S8). All eight of these models had appropriate Bayesian P values (~0.5) indicating model fit and that values calculated from the simulated data are distributed around the observed values (Appendix S2).

Comparison of model types

Each model was built to evaluate commonly used modeling methods (single trait × growth rate models and trait × environment × growth rate models) with high-dimensional models containing a three-way interaction between two functional traits and the environment. Below, we present an extended comparison between simple models and the "full" model for one of the eight different significant three-way interactions found (LMA × RMF × light). We then present just the interpretation of the "full" model for the remaining seven three-way interactions.

The "full" model, which contained the three-way interaction LMA × RMF × light, had equally the highest support (lower DIC) than all iterations of variables of this "full" model (Appendix S2: Table S1). We compared the "full" model with the simplest, commonly used models that fit linear mixed-effects models with relative growth rate (RGR) as a function of each trait. We found significant negative relationships between leaf mass per area (LMA) and RGR (Appendix S1: Table S7) as well as between root mass fraction (RMF) and RGR (Appendix S1: Table S7). However, neither of these models was as well supported as the "full" model based on DIC (Appendix S2: Table S1). Next, we included a trait by environment interaction into the linear mixed-effects models. The interaction between LMA and light was not significant (Fig. 2a) so the first criteria for evidence of growth performance peaks was not met (Fig. 2b). However, the interaction between RMF and light was significant (Fig. 2c), but the slope of the relationship between RMF and RGR had only a few individuals cross zero along the light gradient suggesting a weak interaction. There was one obvious peak in RGR for individuals when they had low RMF in high light environments; however, some individuals did occupy an alternative peak where individuals had high RMF in low light environments (Fig. 2d). Despite these models with two-way interactions showing evidence of growth peaks, they had higher DIC values (less support) than the "full" model that contained the three-way interaction (Appendix S2: Table S1). Furthermore, the single term and two-way interaction term models afforded less interpretation of the effects of the model variables on growth because they lack the three-way interaction term between two traits and the environment.

This "full" model contained a significant interaction between LMA, RMF, and light and had equally the highest support (lowest DIC) following variable selection of the model (Fig. 3a; Appendix S2: Table S1). The slope of the relationship between LMA and RGR at different values of RMF changed sign along the light gradient indicating multiple growth performance peaks, which allows for the effect of the three-way interaction term on growth to be examined. In low light environments, there were two growth performance peaks for individuals, one when they had low LMA and high RMF and one when they had high LMA and low RMF (Fig. 3b). In high light environments, there were also two growth performance peaks for individuals, one when they had both high LMA and RMF and one when they had both low LMA and RMF (Fig. 3b).

Evidence of multiple growth performance peaks

The following three models had a three-way interaction term that was significant in the model and had a slope that changed sign along the environmental gradient (i.e., multiple growth performance peaks present). Variable selection was performed on each model separately using DIC. For each of these models, the "full" model was not the best supported overall, but had higher support than commonly used trait-growth rate and trait × environment × growth rate models (Appendix S2: Tables S6–S8). For each of these three models, the best supported model was a complex model highlighting the inability of simple models to reflect the effects of the traits and the environment on growth (Appendix S2: Tables S6–S8).

The first of these three models had a significant three-way interaction between LMA, stem mass fraction (SMF), and light (Appendix S1: Fig. S2a; Appendix S2: Table S6). For individuals to achieve a growth performance peak across the light gradient, they combined LMA and SMF in different manners (Appendix S1: Fig. S2b). In low light environments, there were two growth performance peaks for individuals, one when they have both low LMA and SMF and one when they have both high LMA and SMF. In high light environments, there were also two growth performance peaks for individuals, one when they have low LMA and high SMF and one when they have high LMA and low SMF. The last two models involved three-way interactions with the soil PC2 environmental variable, which was negatively associated with soil Ca and P. The first involved an interaction between LMA, RMF, and soil PC2 (Appendix S1: Fig. S3a; Appendix S2: Table S7). When soil PC2 was low, indicating high levels of Ca and P, plants with high LMA and low RMF or low LMA and high RMF grew faster (Appendix S1: Fig. S3b). In high soil PC2 environments, indicating low levels of Ca and P, plants with either low LMA and low RMF or high LMA and high RMF performed best (Appendix S1: Fig. S3b). Finally, there was a significant interaction between leaf area ratio (LAR) and leaf mass fraction (LMF) (Appendix S1: Fig. S4a; Appendix S2: Table S8). We found that the effect of LAR on growth rates along the soil PC2 gradient was dependent on LMF (Appendix S1: Fig. S4b). In order for individuals to be
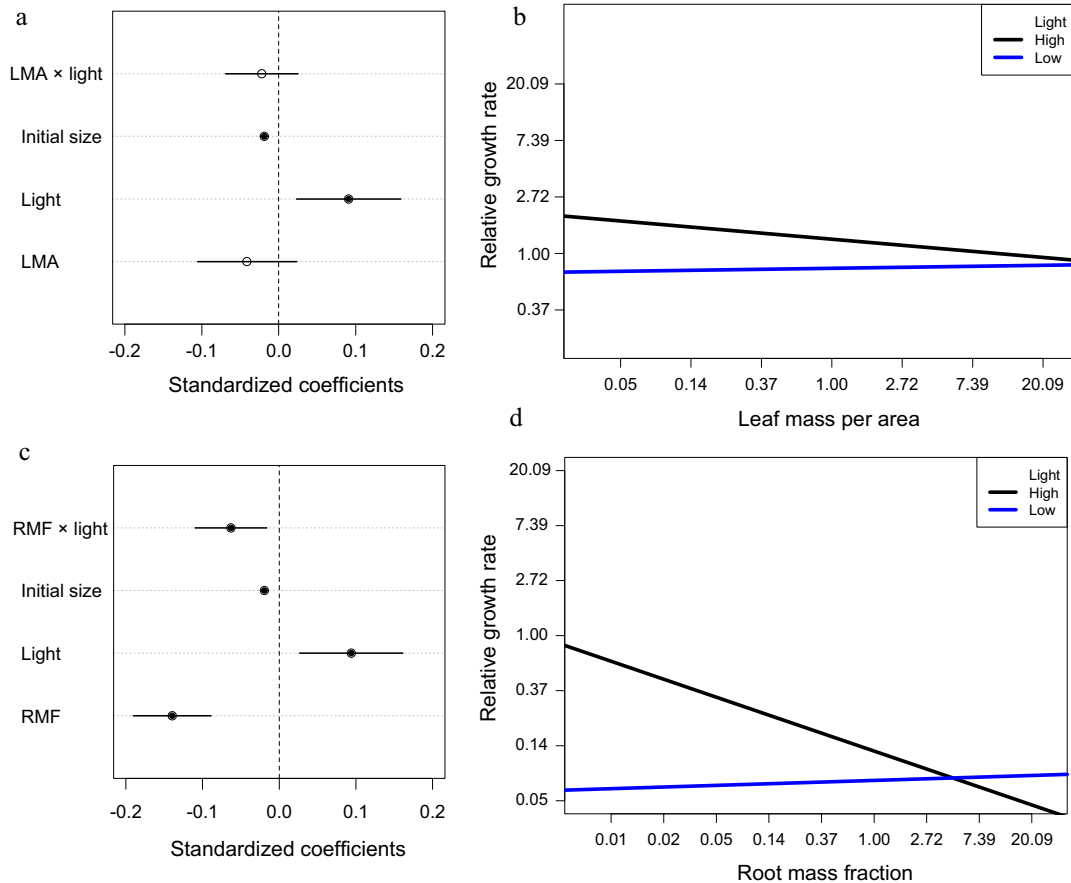
FIG. 2. Models including two-way interactions between (a, b) leaf mass per area (LMA) and light and between (c, d) root mass fraction (RMF) and light. (a,c) Standardized regression coefficients where circles indicate posterior mean values, lines indicate 95% credible intervals, and solid circles represent significant effects. (b) Simple slopes and intercepts visualizing the partial effects of LMA on RGR when light is held constant at its minimum (0.66) and maximum values (10.10). d) Simple slopes and intercepts visualizing the partial effects of RMF on RGR when light is held constant at its minimum (0.66) and maximum (10.10) values. All variables were ln-transformed and scaled to unit variance. Values on the axes have been back transformed.

on a growth performance peak in low soil PC2 environments, meaning high Ca and P, they had high LAR and low LMF or high LAR and high LMF (Appendix S1: Fig. S4b). However, we were unable to statistically show each of these peaks separately because the slopes for each peak were the same sign since LAR was high for both peaks. In high soil PC2 environments, individuals with high LAR and high LMF or low LAR and low LMF exhibited peak growth performance (Appendix S1: Fig. S4b).

The "full" model of the remaining four models had the best support or equal support (ΔDIC < 5) after variable selection (Appendix S2: Tables S2–S5). These models also had support for multiple growth performance peaks (i.e., they had a slope that switched sign along the environmental gradient). Three of these models had significant interactions of traits with soil PC1, which was negatively associated with Mg, K, and Zn (Appendix S1: Table S3). The first interaction was between LMA and RMF (Appendix S1: Fig. S5a; Appendix S2: Table S2).

In low soil PC1 environments, indicating high levels of Mg, K, and Zn, individuals had high LMA and low RMF or low LMA and high RMF (Appendix S1: Fig. S5b). In high soil PC1 environments, individuals with high LMA and high RMF or low LMA and low RMF exhibited peak growth performance (Appendix S1: Fig. S5b). The second interaction was between leaf thickness and RMF (Appendix S1: Fig. S6a; Appendix S2: Table S3). In order for individuals to be on a growth performance peak in low soil PC1 environments, they had high leaf thickness and low RMF or low leaf thickness and high RMF (Appendix S1: Fig. S6b). In high soil PC1 environments, individuals with high leaf thickness and high RMF or low leaf thickness and low RMF exhibited peak performance (Appendix S1: Fig. S6b). The next interaction was between leaf thickness and SMF (Appendix S1: Fig. S7a; Appendix S2: Table S4). Two performance peaks were found when soil PC1 is low and when soil PC1 is high (Appendix S1: Fig. S7b). When soil PC1
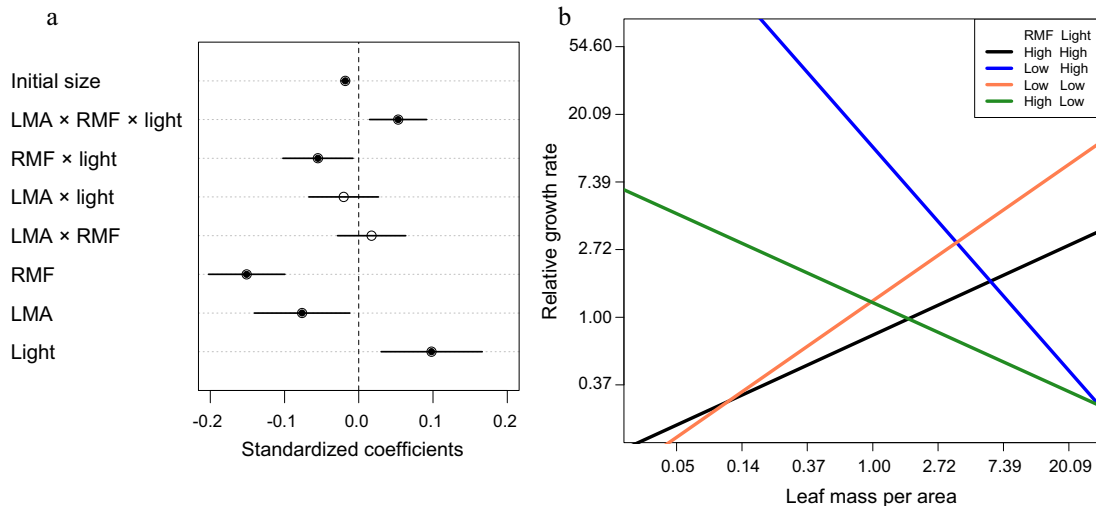
Fig. 3. Model including three-way interaction between leaf mass per area (LMA), root mass fraction (RMF), and light. (a) Standardized regression coefficients where circles indicate posterior mean values, lines indicate 95% credible intervals, and solid circles represent significant effects. (b) Simple slopes and intercepts visualizing the partial effects of LMA on RGR when RMF and light are held constant at combinations of their minimum (RMF = 0.04, light = 0.66) and maximum (RMF = 0.93, light = 10.10) values. All variables were scaled and ln-transformed. Values on the axes have been back transformed. In low light environments, there are two growth performance peaks for individuals, one when they have low LMA and high RMF and one when they have high LMA and low RMF. In high light environments, there are two performance peaks for individuals, one when they have low LMA and low RMF and one when they have high LMA and high RMF.

was low, indicating high levels of Mg, K, and Zn, individuals with low leaf thickness and low SMF or high leaf thickness and high SMF exhibited the highest RGR (Appendix S1: Fig. S7b). When soil PC1 was high, indicating low values of Mg, K, and Zn, individuals with low leaf thickness and high SMF or high leaf thickness and low SMF exhibited peak growth performance (Appendix S1: Fig. S7b). The final model had a significant interaction between leaf thickness, SSL, and soil PC2 (Appendix S1: Fig. S8a; Appendix S2: Table S5). For this interaction of traits, peak growth performance in low soil PC2 environments occurred for individuals that had high leaf thickness with high SSL or had low leaf thickness with low SSL (Appendix S1: Fig. S8b). To perform well in high soil PC2 environments, plants with low leaf thickness and high SSL or high leaf thickness and low SSL had faster growth (Appendix S1: Fig. S8b).

DISCUSSION

Here, we have provided empirical evidence of multiple peaks in growth rate, a strong determinant of long-term plant performance, across phenotypic space in a diverse tropical seedling community, thereby indicating the presence of multiple successful alternative designs. In other words, multiple trait combinations can lead to similar growth performance. The location of growth performance peaks in phenotypic space shifts across local-scale light and soil gradients such that no single or set of interacting traits resulted in a peak in growth across these environmental gradients. These results help to

demonstrate how functional diversity can be maintained in ecological communities and question the practice of utilizing a single trait or environmental variable in isolation to predict the growth performance of individual trees.

Through a step-wise process of increasing model complexity, we have shown that including interactions between two functional traits and the environment and visualization of growth performance landscapes leads to a better overall indication of how functional traits and the environment affect individual seedling growth performance. Specifically, we provide five separate instances where multiple growth performance peaks are found in best supported (ΔDIC < 5) high-dimensional models containing a three-way interaction (Fig. 3, Appendix S1: Figs. S5–S8).

Based on fast-slow plant economics theory (Reich 2014), it may be expected that single growth performance peaks relating to a combination of acquisitive values may be found in areas with higher resource levels. For example, species with relatively more leaf mass investment and lower leaf mass per area (LMA) may be expected in high light environments (Lusk et al. 2008). Similarly, combinations of conservative traits (e.g., low root mass investment and high LMA), may be expected to have superior growth in resource poor (e.g., low light) environments. This expectation is only partially supported by our results. For example, we did find a growth performance peak for plants with acquisitive traits (i.e., relatively high root investment and low LMA) in high soil nutrient environments (Appendix S1: Figs. S3 and

S5). However, we also have several instances where multiple growth performance peaks occur at a given point on light or soil gradients and many of these peaks combine an acquisitive belowground strategy and a conservative aboveground or leaf level strategy. For instance, at the high end of the soil PC1 gradient, meaning low levels of Mg, K, and Zn, growth performance peaked at either high LMA with high root mass fraction (RMF), which reflect a more conservative leaf strategy and acquisitive root strategy, respectively, or low LMA with low RMF, which reflect a more acquisitive leaf strategy and conservative root strategy (Appendix S1: Fig. S5). For the soil nutrient gradients, we found multiple growth performance peaks at both ends of the gradients. The high ends of the soil PC1 and PC2 gradients were associated with low levels of K, Mg, Zn, (PC1) and Ca and P (PC2), nutrients known to play major roles in photosynthesis, growth, as well as seed and stem maturation (Terry and Ulrich 1974, Wissuwa 2003, Wright et al. 2004, Broadley et al. 2007, Holste et al. 2011). Soil moisture may have also contributed to peaks associated with soil nutrients, but we were unable to measure this environmental axis.

This modulation of root and leaf resource acquisition may indicate a fourth interaction between light and soil nutrient levels (Freschet et al. 2015). We did not explicitly test for interactions between environmental gradients here; however, our results generally indicate that aboveground resource levels (i.e., light) and belowground resource levels (i.e., soil nutrients) can vary independently such that mixtures of conservative and acquisitive leaf and root strategies can be selected independently in a forest depending on the resource that is most limiting. Indeed, soil and light variables are very weakly correlated in this study, which likely promotes a greater diversity of trait combinations in the community (Appendix S1: Table S8). We do note that leaf and root traits, at the plant level, are not independent of one another, given that plants only have a finite amount of resources to invest in each. However, we have shown that plants can express acquisitive leaf traits while their root traits are conservative, which may allow us to see disassociation of leaf and root traits at the population or community level. Thus, our results often did not indicate superior growth arising from either conservative or acquisitive strategies at the whole-plant scale and this is likely due to the independence of the selective environments above- and belowground in the system. In other systems where resource levels above- and belowground co-vary, a whole-plant coordination of plant functional spectra may be more common (e.g., Freschet et al. 2015). The results also coincide with evidence in the literature that indicates major functional spectra (e.g., leaf and wood economics spectra; e.g., Baraloto et al. 2010; leaf and root economics spectra; e.g., Fortunel et al. 2012) are generally weakly correlated in adult trees in tropical forests as is the case in the present study for tropical seedlings (Appendix S1: Table S4). All other

significant interactions were similar in that multiple growth performance peaks and frequent independence of above- and belowground strategies were evident (Appendix S1: Figs. S2–S8).

Functional trait-based studies of plant community assembly and structure often focus on abiotic selection for optimal trait values. For example, community weighted mean trait values are expected to shift predictably across abiotic gradients (Muscarella and Uriarte 2016), and the stress gradient hypothesis (Keddy 1992) emphasizes that the expected variation around this trait optimum should decrease in more abiotically stressful conditions (Dwyer and Laughlin 2017b). Correlative studies of plant functional traits and demographic rates implicitly assume that a single trait value will lead to a similar demographic outcome across environments (Laughlin 2018; but see Westerband and Horvitz 2017). This is because of their use of a linear model regressing a trait on a rate using data from many environments or data sets. We have shown empirically that multiple growth performance peaks associated with different trait combinations can occur at multiple points along an environmental gradient. Multiple growth performance peaks were found on both ends of the environmental gradients, indicating that, in extreme ends of an environmental gradient, multiple trait combinations can lead to high demographic performance. Importantly, we show the performance of a single trait value is dependent upon other trait values. Combined, the trait × trait and trait × environment interactions, the context dependencies of trait–performance relationships, and the ability of multiple trait combinations to give rise to similar performance outcomes indicate why single functional traits often fail to predict tree demographic rates (Poorter et al. 2008; Paine et al. 2015, Yang et al. 2018, Swenson et al. 2020) and how trait diversity can be maintained in ecological communities.

High-dimensional trait-based trade-offs have been hypothesized as being important for promoting species coexistence and maintaining community diversity (e.g., Adler et al. 2013, Kraft et al. 2015). Our results support this hypothesis by showing that the relationship between traits, the environment, and demographic outcomes is complex and can lead to alternative phenotypic designs. While we find evidence in this study from multiple models of multiple growth performance peaks, we understand that performance will vary across years and that growth isn't the only metric of performance. We also know that the number of peaks we found is relatively small compared with the number of species in our study system with only eight of 84 models having evidence of multiple growth performance peaks. This raises several new questions that should be addressed in the future. First, how densely occupied are growth performance peaks? Specifically, if multiple peaks exist in phenotypic space, are some more densely occupied by individuals and species in the system and, if so, why? Second, are growth performance peaks mitigated or eroded by other

demographic outcomes (e.g., low survival rates, recruitment or reproductive output) at the same or later life stages such that ultimately a single peak is produced from a given environment? Answering these two questions is critical for our understanding of why trait distributions in tropical forests often have only one or two modes (e.g., Swenson et al. 2012). Final outstanding questions are: how do species that occupy the same growth performance peak co-exist? Are intraspecific interactions (e.g., shared enemies, competition) strong enough to permit the co-existence of multiple species on a given growth performance peak? Do species occupying the same peak spatially or temporally segregate the environment? These questions are all large foundational questions in trait-based community ecology and our results should refocus this literature toward a stronger consideration of performance landscapes and multiple alternative phenotypic designs.

Conclusions

Here we have explored the possibility that multiple growth performance peaks occur in the phenotypic space found in a diverse tropical seedling community using detailed individual-level trait and growth rate data. We find evidence for multiple peaks in phenotypic space and that these peaks shift across environmental gradients. Further, we found evidence that above- and belowground functional strategies often combine to produce optimal growth performance in such a way that acquisitive aboveground strategies can align with conservative belowground strategies and vice versa. Combined, these results show that there are multiple trait combinations possible in phenotypic space that will lead to increased growth performance in a diverse community, which lead to the promotion and maintenance of functional diversity. The results also caution against focusing on single trait analyses in functional trait-based community ecology and the aggregation of individual-level trait variation to the species level. In particular, complex trait × trait and trait × environment interactions are realized at the individual level in communities and performance landscapes should be empirically quantified and conceptualized using individual-level data (Liu et al. 2016, Umaña et al. 2018, Swenson et al. 2020). Last, future research will be needed to uncover the mechanisms that allow multiple species in a community to occupy the same performance peaks in multidimensional phenotypic space and how above- and belowground resource levels interact to influence performance landscapes across systems.

Literature Cited

Ackerly, D. D., et al. 2000. The evolution of plant ecophysiological traits: Recent advances and future directions. BioScience 50:979–995.

Ackerly, D. D. 2003. Community assembly, niche conservatism, and adaptive evolution in changing environments. International Journal of Plant Sciences 164:S165–S184.

Adler, P. B., A. Fajardo, A. R. Kleinhesselink, and N. J. B. Kraft. 2013. Trait-based tests of coexistence mechanism. Ecology Letters 16:1294–1306.

Adler, P. B., R. Salguero-Gómez, A. Compagnoni, J. S. Hsu, J. Ray-Mukherjee, C. Mbeau-Ache, and M. Franco. 2014. Functional traits explain variation in plant life history strategies. Proceedings of the National Academy of Sciences USA 111:740–745.

Anderson, J. T. 2016. Plant fitness in a rapidly changing world. New Phytologist 210:81–87.

Arnold, S. J., M. E. Pfrender, and A. G. Jones. 2001. The adaptive landscape as a conceptual bridge between micro- and macroevolution. Genetica 112–113:9–32.

Baldeck, C. A., et al. 2013. Soil resources and topography shape local tree community structure in tropical forests. Proceedings of the Royal Society B 280:20122532.

Baraloto, C., C. E. T. Paine, L. Poorter, J. Beauchene, D. Bonal, A. Domenach, B. Hérault, S. Patiño, J.-C. Roggy, and J. Chave. 2010. Decoupled leaf and stem economics in rain forest trees. Ecology Letters 13:1338–1347.

Blonder, B., R. E. Kapas, R. M. Dalton, B. J. Graae, J. M. Heiling, and Ø. H. Opedal. 2018. Microenvironment and functional-trait context dependence predict alpine plant community dynamics. Journal of Ecology 106:1323–1337.

Broadley, M. R., P. J. White, J. P. Hammond, I. Zelko, and A. Lux. 2007. Zinc in plant. New Phytologist 173:677–702.

Cao, M., H. Zhu, H. Wang, G. Lan, Y. Hu, S. Zhou, X. Deng, and J. Cui.2008. Xishuangbanna tropical seasonal rainforest dynamics plot: Tree distribution maps, diameter tables and species documentation. Yunnan Science and Technology Press, Kunming, China.

Cavender-Bares, J., D. D. Ackerly, D. A. Baum, and F. A. Bazzaz. 2004. Phylogenetic overdispersion in Floridian oak communities. American Naturalist 163:823–843.

Chave, J., D. Coomes, S. Jansen, S. L. Lewis, N. G. Swenson, and A. E. Zanne. 2009. Towards a worldwide wood economics spectrum. Ecology Letters 12:351–366.

Costa, D. S., F. Gerschlauer, H. Pabst, A. Kühnel, B. Huwe, R. Kiese, Y. Kuzyakov, and M. Kleyer. 2017. Community-weighted means and functional dispersion of plant functional traits along environmental gradients on Mount Kilimanjaro. Journal of Vegetation Science 28:684–695.

D'Andrea, R., A. Ostling, and J. P. O'Dwyer. 2018. Translucent windows: how uncertainty in competitive interactions impacts detection of community pattern. Ecology Letters 21:826–835.

Denwood, M. J. 2016. runjags: An R package providing interface utilities, model templates, parallel computing methods and additional distributions for MCMC models in JAGS. Journal of Statistical Software 71:1–25.

Dwyer, J. M., and D. C. Laughlin. 2017a. Selection on trait combinations along environmental gradients. Journal of Vegetation Science 28:672–673.

Dwyer, J. M., and D. C. Laughlin. 2017b. Constraints on trait combinations explain climatic drivers of biodiversity: the importance of trait covariance in community assembly. Ecology Letters 20:872–882.

Enquist, B. J., A. J. Kerkhoff, S. C. Stark, N. G. Swenson, M. C. McCarthy, and C. A. Price. 2007. A general integrative model for scaling plant growth, carbon flux, and functional trait spectra. Nature 449:218–222.

Enquist, B. J., J. Norberg, S. P. Bonser, C. Violle, C. T. Webb, A. Henderson, L. L. Sloat, and V. M. Savage. 2015. Scaling from traits to ecosystems: Developing a general trait driver theory via integrating trait-based and metabolic scaling theories. Advances in Ecological Research 52:249–318.

Evans, J. R., and V. C. Clarke. 2019. The nitrogen cost of photosynthesis. Journal of Experimental Botany 70:7–15.

Fonseca, C. R., J. M. C. Overton, B. Collins, and M. Westoby. 2000. Shifts in trait-combinations along rainfall and phosphorus gradients. Journal of Ecology 88:964–977.

Fortunel, C., P. V. A. Fine, and C. Baraloto. 2012. Leaf, stem and root tissue strategies across 758 Neotropical tree species. Functional Ecology 26:1153–1161.

Freschet, G. T., E. M. Swart, and J. H. C. Cornelissen. 2015. Integrated plant phenotypic responses to contrasting above- and below-ground resources: key roles of specific leaf area and root mass fraction. New Phytologist 206:1247–1260.

Garnier, E. 1991. Resource capture, biomass allocation and growth in herbaceous plants. Trends in Ecology and Evolution 6:126–131.

Gelman, A., and D. B. Rubin. 1992. Inference from iterative simulation using multiple sequences. Statistical Science 7:457–511.

Gelman, A., X.-L. Meng, and H. Stern. 1996. Posterior predictive assessment of model fitness via realized discrepancies. Statistica Sinica 6:733–807.

Gelman, A., J. B. Carlin, H. S. Stern, D. B. Dunson, A. Vehtari, and D. B. Rubin. 2013. Bayesian data analysis, Third edition. Chapman and Hall/CRC, New York, New York, USA.

Green, P. T., K. E. Harms, and J. H. Connell. 2014. Nonrandom, diversifying processes are disproportionately strong in the smallest size classes of a tropical forest. Proceedings of the National Academy of Sciences USA 111:18649–18654.

Hair, J. F., W. C. Black, B. J. Babin, and R. E. Anderson. 2014. Multivariate data analysis. Seventh edition. Pearson Education Limited, Harlow, UK.

HilleRisLambers, J., P. B. Adler, W. S. Harpole, J. M. Levine, and M. M. Mayfield. 2012. Rethinking community assembly through the lens of coexistence theory. Annual Review of Ecology, Evolution, and Systematics 43:227–248.

Hoffmann, W. A., and H. Poorter. 2002. Avoiding bias in calculations of relative growth rate. Annals of Botany 80:37–42.

Holste, E. K., R. K. Kobe, and C. F. Vriesendorp. 2011. Seedling growth responses to soil resources in the understory of a wet tropical forest. Ecology 92:1828–1838.

Hubbell, S. P., R. B. Foster, S. T. O'Brien, K. E. Harms, R. Condit, B. Wechsler, S. J. Wright, and S. Loo-de-Lao. 1999. Light-gap disturbances, recruitment limitation, and tree diversity in a neotropical forest. Science 283:554–557.

Itoh, A., T. Yamakura, T. Ohkubo, M. Kanzaki, P. A. Palmiotto, J. V. LaFrankie, P. S. Ashton, and H. S. Lee. 2003. Importance of topography and soil texture in the spatial distribution of two sympatric dipterocarp trees in a Bornean rainforest. Ecological Research 18:307–320.

Jager, M. M., S. J. Richardson, P. J. Bellingham, M. J. Clearwater, and D. C. Laughlin. 2015. Soil fertility induces coordinated responses of multiple independent functional traits. Journal of Ecology 103:374–385.

John, R., et al. 2007. Soil nutrients influence spatial distributions of tropical tree species. Proceedings of the National Academy of Sciences USA 104:864–869.

Keddy, P. A. 1992. Assembly and response rules: two goals for predictive community ecology. Journal of Vegetation Science 3:157–164.

Kéry, M. 2010. Introduction to WinBUGS for ecologists. Academic Press, Burlington, Vermont, USA.

Kraft, N. J. B., M. R. Metz, R. S. Condit, and J. Chave. 2010. The relationship between wood density and mortality in a global tropical forest data set. New Phytologist 188:1124–1136.

Kraft, N. J. B., O. Godoy, and J. M. Levine. 2015. Plant functional traits and the multidimensional nature of species coexistence. Proceedings of the National Academy of Sciences USA 112:797–802.

Laughlin, D. C. 2018. Rugged fitness landscapes and Darwinian demons in trait-based ecology. New Phytologist 217:501–503.

Laughlin, D. C., and J. Messier. 2015. Fitness of multidimensional phenotypes in dynamic adaptive landscapes. Trends in Ecology and Evolution 30:487–496.

Laughlin, D. C., R. T. Strahan, P. B. Adler, and M. M. Moore. 2018. Survival rates indicate that correlations between community-weighted mean traits and environments can be unreliable estimates of the adaptive value of traits. Ecology Letters 21:411–421.

Lesaffre, E., and A. B. Lawson. 2012. Bayesian biostatistics. John Wiley & Sons, West Sussex, UK.

Liu, X., N. G. Swenson, D. Lin, X. Mi, M. N. Umaña, B. Schmid, and K. Ma. 2016. Linking individual-level functional traits to tree growth in a subtropical forest. Ecology 97:2396–2405.

Lusk, C. H., P. B. Reich, R. A. Montgomery, D. D. Ackerly, and J. Cavender-Bares. 2008. Why are evergreen leaves so contrary about shade? Trends in Ecology and Evolution 23:299–303.

Marks, C. O., and M. J. Lechowicz. 2006. Alternative designs and the evolution of functional diversity. American Naturalist 167:55–66.

McGill, B. J., B. J. Enquist, E. Weiher, and M. Westoby. 2006. Rebuilding community ecology from functional traits. Trends in Ecology and Evolution 21:178–185.

Metz, M. R., W. P. Sousa, and R. Valencia. 2010. Widespread density-dependent seedling mortality promotes species coexistence in a highly diverse Amazonian rain forest. Ecology 91:3675–3685.

Muscarella, R., and M. Uriarte. 2016. Do community-weighted mean functional traits reflect optimal strategies? Proceedings of the Royal Society B 283:20152434.

Ohlemüller, R., S. Walker, and J. B. Wilson. 2006. Local vs regional factors as determinants of the invasibility of indigenous forest fragments by alien plant species. Oikos 112:493–501.

Onoda, Y., et al. 2011. Global patterns of leaf mechanical properties. Ecology Letters 14:301–312.

Paine, C. E. T., et al. 2015. Globally, functional traits are weak predictors of juvenile tree growth, and we do not know why. Journal of Ecology 103:978–989.

Paine, C. E. T., M. Stenflo, C. D. Philipson, P. Saner, R. Bagchi, R. C. Ong, and A. Hector. 2012. Differential growth responses in seedlings of ten species of Dipterocarpaceae to experimental shading and defoliation. Journal of Tropical Ecology 28:377–384.

Palmiotto, P. A., S. J. Davies, K. A. Vogt, M. S. Ashton, D. J. Vogt, and P. S. Ashton. 2004. Soil-related habitat specialization in dipterocarp rain forest tree species in Borneo. Journal of Ecology 92:609–623.

Plummer, M. 2003. JAGS: A program for analysis of Bayesian graphical models using Gibbs sampling. Pages 1–10 in *K. Hornik, F. Leisch, and A. Zeileis, editors. Proceedings of the 3rd International workshop on distributed statistical computing (DSC 2003). Austrian Association for Statistical Computing (AASC) and the R Foundation for Statistical Computing, Vienna, Austria.*

Plummer, M. 2016. rjags: Bayesian graphical models using MCMC. R package version 4-6. https://CRAN.R-project.org/package=rjags

Poorter, L., et al. 2008. Are functional traits good predictors of demographic rates? Evidence from five neotropical forests. Ecology 89:1908–1920.

Poorter, H., K. J. Niklas, P. B. Reich, J. Oleksyn, P. Poot, and L. Mommer. 2012. Biomass allocation to leaves, stems and roots: meta-analyses of interspecific variation and environmental control. New Phytologist 193:30–50.

R Development Core Team. 2016. R: a language and environment for statistical computing. R Foundation for Statistical Computing, Vienna, Austria. https://www.R-project.org/

Reich, P. B. 2014. The world-wide 'fast-slow' plant economics spectrum: a traits manifesto. Journal of Ecology 102:275–031.

Reich, P. B., M. B. Walters, and D. S. Ellsworth. 1997. From tropics to tundra: Global convergence in plant functioning. Proceedings of the National Academy of Sciences USA 94:13730–13734.

Russo, S. E., S. J. Davies, D. A. King, and S. Tan. 2005. Soil-related performance variation and distributions of tree species in a Bornean rain forest. Journal of Ecology 93:879–889.

Russo, S. E., P. Brown, S. Tan, and S. J. Davies. 2008. Interspecific demographic trade-offs and soil-related habitat associations of tree species along resource gradients. Journal of Ecology 96:192–203.

Simpson, G. G. 1944. Tempo and mode in evolution. Columbia University Press, New York, New York, USA.

Spiegelhalter, D. J., N. G. Best, B. P. Carlin, and A. Van Der Linde. 2002. Bayesian measures of model complexity and fit. Journal of the Royal Statistical Society Series B: Statistical Methodology. 64:583–616.

Swenson, N. G., et al. 2012. The biogeography and filtering of woody plant functional diversity in North and South America. Global Ecology and Biogeography 21:798–808.

Swenson, N. G., S. J. Worthy, D. Eubanks, Y. Iida, L. Monks, K. Petprakob, V. E. Rubio, K. Staiger, and J. Zambrano. 2020. A reframing of trait-demographic rate analyses for ecology and evolutionary biology. International Journal of Plant Sciences 181:33–43.

Terry, N., and A. Ulrich. 1974. Effects of magnesium deficiency on the photosynthesis and respiration of leaves of sugar beet. Plant Physiology 54:379–381.

Umaña, M. N., C. Zhang, M. Cao, L. Lin, and N. G. Swenson. 2015. Commonness, rarity, and intraspecific variation in traits and performance in tropical tree seedlings. Ecology Letters 18:1329–1337.

Umaña, M. N., J. Forero-Montaña, R. Muscarella, C. J. Nytch, J. Thompson, M. Uriarte, J. Zimmerman, and N. G. Swenson. 2016. Interspecific functional convergence and divergence and intraspecific negative density dependence underlie the seed-seedling transition in tropical trees. American Naturalist 187:99–109.

Umaña, M. N., E. F. Zipkin, C. Zhang, M. Cao, L. Lin, and N. G. Swenson. 2018. Individual-level trait variation and negative density dependence affect growth in tropical tree seedlings. Journal of Ecology 106:2446–2455.

Westerband, A. C., and C. C. Horvitz. 2017. Early life conditions and precipitation influence the performance of widespread understorey herbs in variable light environments. Journal of Ecology 105:1298–1308.

Wissuwa, M. 2003. How do plants achieve tolerance to phosphorus deficiency? Small causes with big effects. Plant Physiology 133:1947–1958.

Wright, S. 1931. Evolution in Mendelian populations. Genetics 16:97–159.

Wright, S. 1932. The roles of mutation, inbreeding, crossbreeding, and selection in evolution. Proceedings of the Sixth International Congress of Genetics 1:356–366.

Wright, S. 1945. Tempo and mode in evolution: a critical review. Ecology 26:415–419.

Wright, I. J., et al. 2004. The worldwide leaf economics spectrum. Nature 428:821–827.

Wright, I. J., and M. Westoby. 1999. Differences in seedling growth behavior among species: trait correlations across species, and trait shifts along nutrient compared to rainfall gradients. Journal of Ecology 87:85–97.

Yang, J., M. Cao, and N. G. Swenson. 2018. Why functional traits do not predict trait demographic rates. Trends in Ecology and Evolution 33:326–336.

SUPPORTING INFORMATION

Additional supporting information may be found in the online version of this article at http://onlinelibrary.wiley.com/doi/10.1002/ecy.3007/suppinfo

DATA AVAILABILITY

All code and data associated with this study are available from http://doi.org/10.5281/zenodo.3382271